Chromatographia (2021) 84:335–345
https://doi.org/10.1007/s10337-020-04001-y

ORIGINAL

Performance Evaluation of Fixed Bed Column Packed with Ionic Liquid Impregnated Silica for Separation of Gadolinium and Neodymium from Aqueous Solutions

H. A. Ibrahim[1] · S. S. Metwally[1] · W. R. Mohamed[1] · E. A. El-Sherief[1] · H. S. Mekhamer[1] · Islam M. I. Moustafa[2] · E. M. Mabrouk[2]

Received: 14 July 2020 / Revised: 20 December 2020 / Accepted: 23 December 2020 / Published online: 3 February 2021

Abstract

Application of fixed bed column for separation of gadolinium and neodymium ions from their aqueous solutions using cyphos IL-104 impregnated silica was investigated. The performance of separation of the two lanthanide elements was evaluated by determining the column capacity, the total quantity sorbed of metal ions, and the removal percentage. These indicative column performance parameters were evaluated in altered conditions including fixed bed height of 2.0 and 3.0 cm, flow rate of 1.0 and 2.0 mL/min, and solution feed concentration of 50 and 100 ppm. Breakthrough modeling of the sorption process across the column was performed by employing Thomas and Adams–Bohart models. It was found that it took less time to reach the breakthrough when the flow rate and initial concentration increased, while the height of the bed decreased. Also, the column capacity increased by increasing the bed depth, decreasing the flow rate, and increasing the initial metal ion concentrations. 0.1 M nitric acid was found to be the best media for the separation of Nd^{3+} and Gd^{3+} ions.

Keywords Separation · Impregnation · Nd^{3+} and Gd^{3+} · Fixed bed column · Modeling

Introduction

The batch technique is important in providing information about the efficiency of metal-sorbent system, but the obtained data are not sufficient for applying this technique to a large scale in the most treatment processes, specially, in continuous-flow mode. Therefore, this study is interested in using the column technique for separation of gadolinium and neodymium ions from their aqueous solutions.

Lanthanide elements enter the environment via various pathways due to the rapid increase of the use of their resources and applications in several fields of modern industry and daily life. Toxicological research has shown that lanthanides can have serious harmful effects on living organisms [1]. In environmental studies, Lanthanides' deposition in water, food chain, and soil must be regarded [2]. Radioisotope of neodymium (light lanthanide element) is used to monitor nuclear fuel utilization [3], as well as its applications in coloring glass, doping glass, lasers, and many electronic devices [4]. Gadolinium (heavy lanthanide element) is used in the nuclear power plant as shielding device to minimize the interaction of thermal neutrons with materials. Gadolinium has application in radiochemical analysis in the determination of the extent of burn-up of nuclear fuels (as ^{154}Gd-^{157}Gd) [5]. Also enters in various applications like lamp phosphors, optical glass, and permanent magnets [6, 7]. Separating and recycling lanthanide components from nuclear and industrial waste are critical for both environment and economy [8–11]. There are different technologies or processes used for radioactive waste treatment based on achieving these goals such as adsorption, chemical precipitation, solvent extraction, membrane process, and ion exchange [12–21]. Sometimes, a combination of several processes can be used to provide effective treatment of a liquid waste stream. Immobilizing an extractant in a resin support allows maintaining their high recovery efficiency

✉ H. A. Ibrahim
haneenabi@yahoo.com

✉ S. S. Metwally
sicosad@hotmail.com

1 Hot Laboratories Center, Egyptian Atomic Energy Authority, Cairo 13759, Egypt

2 Chemistry Department, Faculty of Science, Banha University, Banha, Egypt

and preventing their dispersion in the aqueous solution (expensive and hazardous compounds) [22]. Additionally, the presence of the resin may enhance the removal efficiency of the extractant [23].

Recovery of solvent extractant immobilized sorption in a fixed bed is an unsteady-state process, involving the accumulation of solute molecules onto a sorbent from a solvent crossing the column.

Sorption using a fixed bed is broadly used in practical industrial applications for purification and separation purposes. The performance of fixed bed column is evaluated by testing the breakthrough curve of the sorption. To explain and forecast the breakthrough curves, a number of mathematical models have been established [24].

This work focused on evaluation of performance of fixed bed column for removal and separation of neodymium and gadolinium ions from aqueous solution. The studied fixed bed column is packed with Cyphos IL-104 impregnated on silica. Thomas and Adams–Bohart models were used to accomplish this evaluation.

Experimental

Materials and Methods

Ionic liquid, namely trihexyl (tetradecyl) phosphonium bis-2, 4,4-(trimethylpentyl) phosphinate, Cyphos IL-104, was purchased from Fluka. Grade 62 Silica gel, 150 Å was obtained from Sigma-Aldrich. NH_4OH, HNO_3, and HCl from Winlab. Neodymium and Gadolinium nitrates from Merck. Chemicals and reagents are of analytical grade.

Column System

The dimensions of the glass column used in this study were 15 cm length and 1 cm inner diameter. A 2.0 mm-thick disc of glass wool is incorporated in the bottom and the top of the column to prevent leakage. For the accuracy of the results, this glass wool verified not to adsorb any weighty amounts of the metal ions from the solution. Impregnated silica, cyphos@silica, was used as a sorbent material. The material was prepared as the same description illustrated in our previous work [2]; where silica was impregnated by an ionic liquid, Cyphos IL-104, as follows: 50% loading percent was achieved by adding 2.0 mL of Cyphos IL-104 to 4 g of silica followed by stirring overnight in the presence of ethanol (few drops). The resulting homogenous mixture was filtered followed by washing with distilled water to eliminate excess solvent. The product (cyphos@silica) was subjected to overnight drying in an air oven at temperature of 333 ± 1 K. The resin (cyphos@silica) was packed through the column. The column was routinely preconditioned with water at a definite flow rate [25]. The metal ion solutions, at optimum pH equals 3.5, were fed into the column. The feeding flow rate was adjusted by a pump connected to the column. The effluent volumes passed throughout the column were collected in known fraction volumes for spectrophotometric measurements. The separation experiment of the two metal ions from their binary solutions was carried out at defined flow rate and bed size. Different concentrations of nitric acid were tested for the elution to find out the optimum concentration for the separation of the two studied Nd^{3+} and Gd^{3+} ions.

Results and Discussion

From the previous work, batch equilibrium results [2], it is clear that both neodymium and gadolinium ions can be effectively removed from aqueous solution by Cyphos@silica material. The sorption using column technique was investigated to evaluate the practical usefulness of Cyphos@silica material for sorption of neodymium and gadolinium from their solutions. The fixed bed column performance presented using breakthrough curves. The breakthrough curve display concentration ratios C_t/C_0 as a function of effluent volumes (C_v), mg/L where C_t is the effluent concentration of neodymium and gadolinium and C_0, mg/L is the initial concentration. When the concentration of effluent, C_t, is equal to that of feed concentration, C_0 (i.e., $C_t/C_0 = 1$) that is an indication of reaching saturation of the column [26]. The column beads were pre-conditioning by washing them with 100 mL distilled water to remove all air bubbles from the column bed. After that, the neodymium and gadolinium solutions passing through the column at optimum pH = 3.5 deduced from batch results [2]. The column performance can be investigated by studying some factors, such as height of the fixed bed, flow rate, and the initial concentration of metal ion solution [27, 28].

Effect of Bed Depth

Different bed depths of 2 and 3 cm were used to investigate the effect of bed depth on the breakthrough curves for Nd^{3+} and Gd^{3+} ion sorption onto Cyphos@silica material. In these investigations, the flow rate and initial feed concentration were fixed to 1 mL/min and 100 mg/L, respectively, for each metal ions solution. The column bed depth of 2.0 and 3.0 cm could be employed by packing the column with 0.79 and 1 gm of Cyphos@silica material, respectively. The total quantity sorbed of metal ions (q_{tot}, mg) in the column, for a specified feed concentration (C_0, mg/L) and flow rate (Q, mL/min) with the total flow time (t_{tot}, min), can be obtained by estimating the area under the breakthrough curve that represents the integration of the sorbed ion concentration

(C_{ads}, mg/L) plotted versus time as presented in the consequent equation [29]:

$$q_{tot} = \frac{Q}{1000} \int_{t=0}^{t=tot} C_{ads}\, dt = \frac{Q}{1000} \int_{t=0}^{t=tot} \left(C_0 - C\right) dt. \quad (1)$$

The total amount of metal ions served to the column (X, mg) is calculated from the next equation:

$$X = \frac{C_0\, V_{eff}}{1000}, \quad (2)$$

where V_{eff} is the volume of the effluent, mL. Ultimate uptake (or bed capacity of the column, mg/g) is defined as: the total amount of metal sorbed, q_{tot} per weight of sorbent, w, for the whole operation time as demonstrated by Eq. (3), and the percent column performance, % can be assessed from Eq. (4):

$$\text{Bed capacity} = \frac{q_{tot}}{w} \quad (3)$$

$$\text{Column performance } (\%) = \frac{q_{tot}}{X} \times 100. \quad (4)$$

Figure 1 illustrates that the shape of breakthrough curve differs with varying the bed depth. The bed capacity, breakthrough time, and the removal percent of Nd^{3+} and Gd^{3+} ions (column performance) increased with increasing the bed depth, as shown in Table 1. The increases in the sorbent doses in longer bed heights lead to increase in the bed capacity in longer bed heights, where higher surface area provided and consequently more sorption sites offered to the metal ions. The bed capacity for Gd^{3+} is greater than Nd^{3+}; this may be due to the difference the ionic radius. Consequently, gadolinium ions (the smaller) can be easily sorbed than neodymium ions.

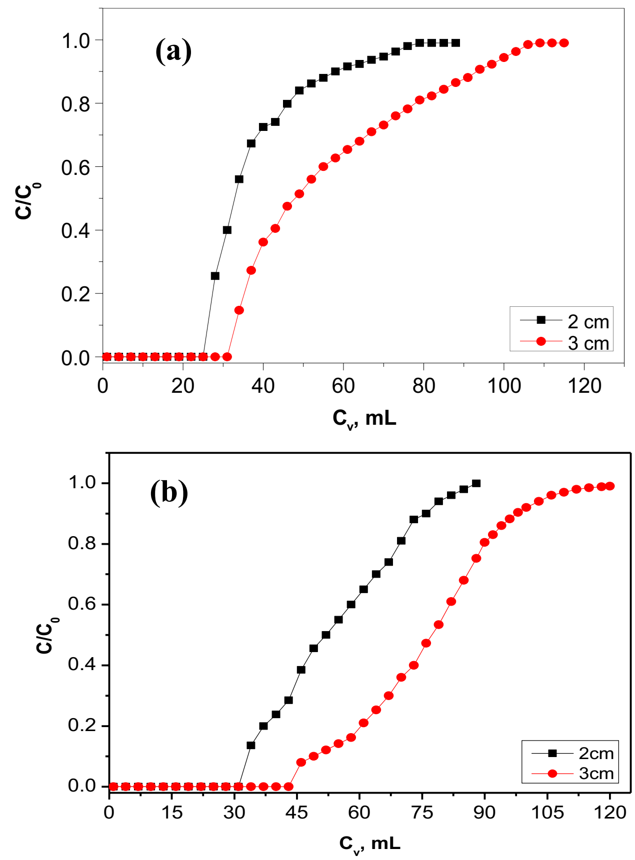

Fig. 1 Effect of bed depth on the breakthrough curve for sorption of **a** Nd^{3+} and **b** Gd^{3+} ions at flow rate 1.0 mL/min and initial concentration 100 mg/L

Effect of Flow Rate

The influence of variable flow rate on sorption of Nd^{3+} and Gd^{3+} ions by Cyphos@silica material was investigated at different flow rates, 1.0 and 2.0 mL/min, whereas keeping the initial metal ion concentration at 100 mg/L and the bed depth of 3 cm. The plots of the breakthrough curves of Nd^{3+} and Gd^{3+} ions at the two flow rates are displayed in Fig. 2. The total sorbed ion quantities and column performance with respect to the two examined flow rates were estimated from the breakthrough curves and are listed in Table 2. From the data obtained, it was found that breakthrough curves become sharper at higher flow rates. With rising flow rate, the breakthrough time and the entire Nd^{3+} and Gd^{3+} ions sorbed decreased. This is certainly due to the reduced contact time that causes a weak distribution of the solution throughout the column, resulting in a lower diffusion of the solution onto the Cyphos@silica material particles.

Initially, the sorption was fast at a lower flow rate likely associated with the availability of reaction sites capable of capturing metal ions around or within the material particles. Due to the incremental occupation of these sites, the opportunity for sorption uptake becomes fewer in the next stage of the process.

When the flow rate is increased, the breakthrough curve becomes steeper with which the breakpoint time and concentration of adsorbed ions decreases. This may explain the reason why the column performance is better at the slowest flow rate [30].

Influence of Initial Feed Concentration

Two initial Nd^{3+} and Gd^{3+} ion concentrations were used for studying the sorption performance of Cyphos@silica column. The effect of varying the initial metal ion concentrations of 50 and 100 mg/L at a flow rate of 1.0 mL/min and bed depth of 3.0 cm is illustrated in Fig. 3. The total sorbed quantities and the removal percent (column performance)

Table 1 Effect of bed depth on breakthrough capacity of Cyphos@silica for sorption of Nd^{3+} and Gd^{3+}

Metal ion	C_0 (mg/L)	Q (mL/min)	Z (cm)	X (mg)	q_{tot} (mg)	Column performance (%)	Bed capacity (mg/g)
Gd^{3+}	100	1	3	12	7.6	63.3	7.6
	100	1	2	10.3	5.38	50.2	6.8
Nd^{3+}	100	1	3	11.2	5.4	48.2	5.4
	100	1	2	8.77	3.76	42.9	4.8

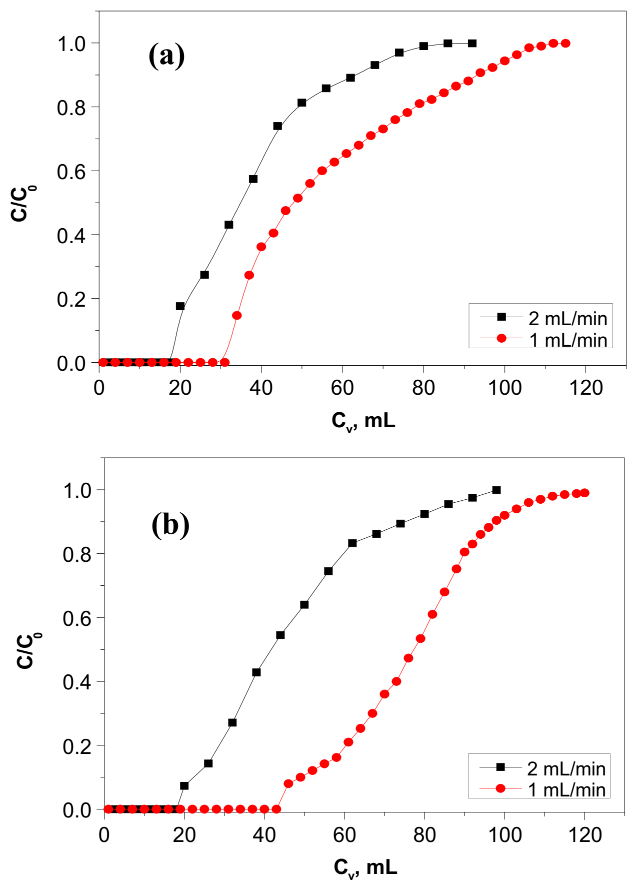

Fig. 2 Effect of flow rate on the breakthrough curve for sorption of **a** Nd^{3+} and **b** Gd^{3+} ions at bed depth 3.0 cm and concentration 100 mg/L

regarding the initial metal ions concentration were calculated and are represented in Table 3. As it is obvious from the figures, the increase in the initial Gd^{3+} and Nd^{3+} concentrations leads to reduction in the amount of solutions treated before breakthrough. This is because column bed saturated by the high concentration of metal ions. Concentration gradient between the concentration of metal ions in the bulk solution and in/inside the sorbent particles considered to be the essential forces that promote the sorption process. This may clarify the reason for acquiring greater sorption capacity of Nd^{3+} and Gd^{3+} at greater concentration of their solution fed to the column [31].

Modeling of Breakthrough Curves

Adams–Bohart Model

Adams–Bohart model [32] relies on the mechanism of reactions that occur on the surface. This model assumes first-order rate of reaction with respect to both solution concentration and free sites on the surface of sorbent. The adsorption rate is proportional to the adsorbent's available vacant sites. The equations describe the relation between normalized concentration (C_t/C_0) and time could be described by this model. The application of the model is constrained on the first portion of the breakthrough curve. The kinetic and ultimate capacity parameters denoted by the symbols k_{AB} and N_0 can be assessed using the following expression:

$$\ln \frac{C_t}{C_0} = k_{AB} C_0 t - k_{AB} N_0 \frac{Z}{F}, \tag{5}$$

where the concentration of the solution fed to and exiting the column is C_0 and C_t (mg/L). k_{AB} (L mg^{-1} min^{-1}) is the

Table 2 Effect of flow rate on breakthrough capacity for sorption of Nd^{3+} and Gd^{3+} onto Cyphos@silica

Metal ion	C_0 (mg/L)	Q (mL/min)	Z (cm)	X (mg)	q_{tot} (mg)	Column performance (%)	Bed capacity (mg/g)
Gd^{3+}	100	1	3	12	7.6	63.3	7.6
	100	2	3	9.8	3.7	37.7	3.7
Nd^{3+}	100	1	3	11.2	5.4	48.2	5.4
	100	2	3	9.21	3.76	40.8	3.5

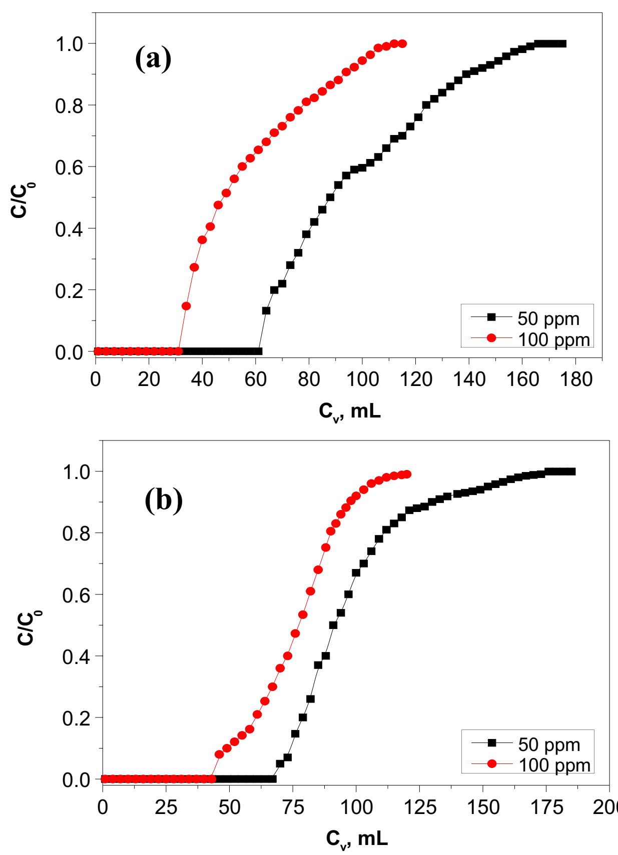

Fig. 3 Effect of initial feed concentration on the breakthrough curve for sorption of **a** Nd^{3+} and **b** Gd^{3+} ions at bed depth 3.0 cm and flow rate 1.0 mL/min

kinetic constant, *F*, cm/min is the linear velocity, *Z*, cm is the column bed height, and N_0, mg/L is the maximum concentration. The validity of this model is restricted to the outlined conditions [33]. The values of N_0 and k_{AB} can be gotten from the intercept and slope the linear plot of ln(C_t /C_0) against time t as represented by Figs. 4, 5, and 6. The calculated values of these and the fitting correlation coefficients exist in Table 4.

As the data in Table 4 show, the values of k_{AB} increases with increasing the flow rate, but it is lessened with increasing bed height and the inlet concentration. The values of N_0 increase with increasing the inlet concentration and bed height but decreasing with speeding the flow rate.

Thomas Model

The Thomas model is a common model that is broadly used for theoretical description of column performance. According to the assumption, axial and radial dispersion are neglected. It also assumes that the physical properties of both the sorbent and the solution do not change during the experiment [34]. The linearized formula of Thomas model can be expressed as follows:

$$\ln\left(\frac{C_0}{C_t} - 1\right) = \frac{k_{Th} q_0 M}{F} - \frac{k_{Th} C_0 V}{F}, \qquad (6)$$

where k_{Th}, mL/min.mg is the Thomas rate constant; q_0, mg/g is the metal ions uptake per g of the adsorbent at equilibrium; C_0 (mg/L) is the influent metal ion concentration; C_t (mg/L) is the outlet concentration at certain time, *t*; *M* (g) is the mass of sorbening material; *F*, (mL min^{-1}) is the flow rate; and *V* (ml) is the throughput volume. The value of C_t/C_0 is the proportion of outlet and influent ion concentrations. A linear plot of ln(C_0/C_t) − 1 versus effluent volume (V_{eff}) was drawn to determine the values of k_{Th} and q_0 from the slope and intercept of the plot as displayed by Figs. 7, 8, and 9. The values of concentration variance obtained from column experiments were fitted to the Thomas model. The constants, k_{Th} and q_0, resulting from linear fitting are presented in Table 5.

From Table 5, it is realized that values of R^2 range from 0.93 to 0.98. Moreover, as the influent concentration increased, the value of q_0 and k_{Th} increased. This increase is due to concentration gradient, while decreasing the values of q_0 was observed when reducing the inlet solution flow rate. As the bed heights increased, the values of q_0 increased and k_{Th} decreased. It is also interestingly observed from the data summarized in Table 5, the q_0 values calculated from the Thomas model is very close to the experimental termed as $q_{c\,(exp)}$. These findings proved the appropriateness of Thomas model for acquiring the sorption processes where the external and internal diffusions will not be the limiting step [35].

Table 3 Effect of initial feed concentration on breakthrough capacity for sorption of Nd^{3+} and Gd^{3+} onto cyphos@silica

Metal ion	C_0 (mg/L)	Q (mL/min)	Z (cm)	X (mg)	q_{total} (mg)	Column performance (%)	Bed capacity (mg/g)
Gd^{3+}	50	1	3	9.2	4.86	52.7	4.86
	100	1	3	12	7.6	63.3	7.6
Nd^{3+}	50	1	3	8.3	4.5	54	4.5
	100	1	3	11.2	5.4	48.2	5.4

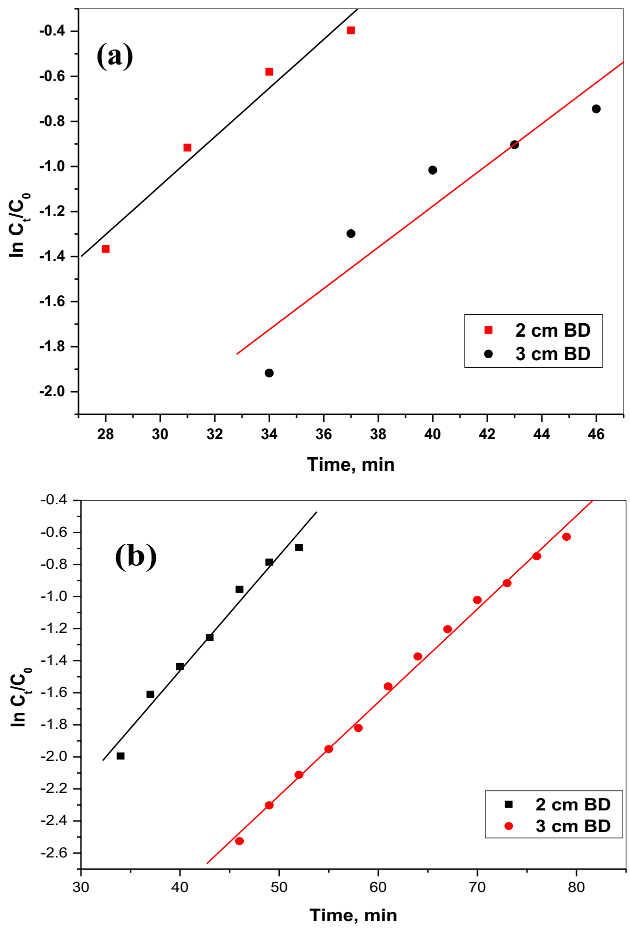

Fig. 4 Adams–Bohart model plots for sorption of **a** Nd^{3+} and **b** Gd^{3+} onto cyphos@silica at various bed depths

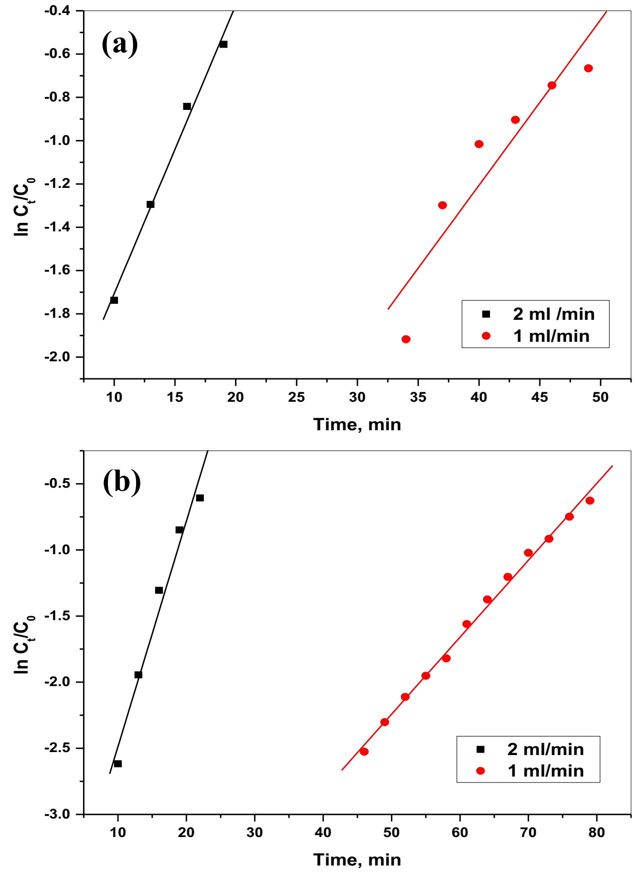

Fig. 5 Adams–Bohart model plots for sorption of **a** Nd^{3+} and **b** Gd^{3+} onto cyphos@silica at different flow rates

Comparison of Batch and Fixed Bed Kinetics of Sorption Process

Batch and column experiments are commonly performed for determining the characteristics of the materials used as sorbents and for evaluation of the whole sorption process. In practical applications, the sorption process may be performed as batch or dynamic continuous operation. The two operations have many advantages in common such as simple to operate and ability of using a wide variety of media, but column operation can be operated at elevated temperatures and offer the advantage of reaching high decontamination factor. Column process may be considered as series of batch operations and such system used frequently in treating radioactive liquid wastes [36, 37].

Kinetics data of sorption of Gd^{3+} and Nd^{3+} in batch mode investigated in our previous work [2] have been tested to Thomas and Adams–Bohart models (Figs. 10, 11). Modified equation of Thomas model for batch adsorption [38] is expressed as follows:

$$\frac{C}{C_0} = \exp\left(k_{\mathrm{Th}}\left(\frac{1-\varepsilon}{\varepsilon}\ \rho\ q_0 - C_0\right)t\right), \tag{7}$$

where ρ is the density of the sorbent material and ε is the liquid volume fraction. The tested sorption data of Gd^{3+} and Nd^{3+} onto the impregnated silica could not fit this form of Thomas model.

Adams–Bohart model rate model relies on surface reaction mechanism. This model assumes first order of reaction with respect to both solution concentration and free sites on the surface of sorbent [39]. Loebenstein et al. [40, 41] develop a solution of both rate and mass conservation equation:

$$C = C_0 - C_0 A\left[\frac{1-\exp\left[(A-1)C_0 k_{\mathrm{AB}}\ t\right]}{1-A\ \exp\left[(A-1)C_0 k_{\mathrm{AB}}\ t\right]}\right], \tag{8}$$

where

$$A = \frac{M q_0}{V C_0}. \tag{9}$$

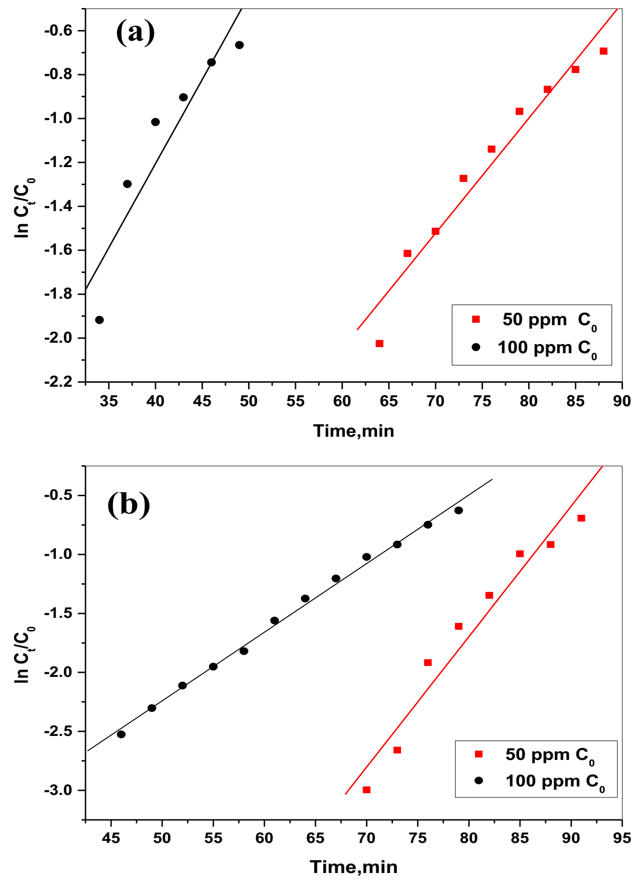

Fig. 6 Adams–Bohart model plots for sorption of **a** Nd^{3+} and **b** Gd^{3+} onto cyphos@silica at initial feed concentrations

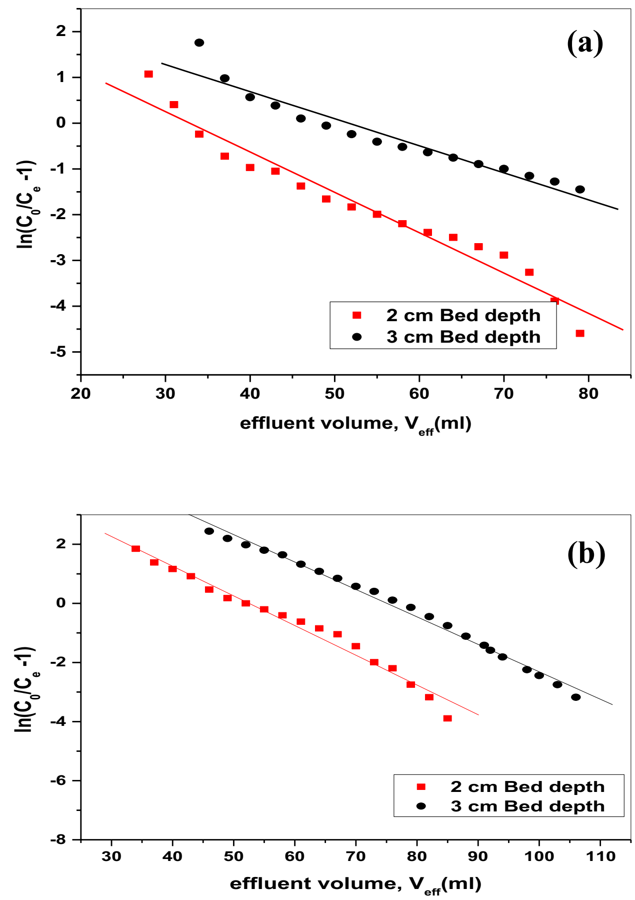

Fig. 7 Thomas model plots for sorption of **a** Nd^{3+} and **b** Gd^{3+} onto cyphos@silica at different bed depths

Table 4 Linear regression analysis of sorption data of Nd^{3+} and Gd^{3+} onto Cyphos@silica fitted to Adam's–Bohart model

C_0(mg/L)	Z (cm)	v (mL/min)	K_{AB} (L mg^{-1} min^{-1})	N_0(mg/L)	R^2
Nd^{3+}					
100	2	1	0.00128	2438	0.99
100	3	1	0.00051	2568	0.95
100	3	2	0.00133	1937	0.99
50	3	1	0.00076	2367	0.95
Gd^{3+}					
100	2	1	0.00072	3735	0.98
100	3	1	0.00058	4416	0.99
100	3	2	0.00171	2088	0.97
50	3	1	0.00058	4053	0.95

Equation in linear form could be expressed as follows:

$$\frac{1}{(A-1)C_0} \ln\left(\frac{(A-1)C_0 + C}{A\ C}\right) = k_{AB}\ t. \tag{10}$$

Plotting of the left-hand side of Eq. (10) vs t should be linear with slope of k_{AB}, rate constants, and maximum capacities of sorption of the impregnated silica toward both metal ions (Table 6).

It can be noticed from the predicted kinetic data by Adams–Bohart model that sorption rate of batch mode sorption is higher than that of sorption by continuous mode using fixed bed column. This may be because the agitation applied during batch experiment led to break of the boundary layer around the sorbent particles.

Separation of Gadolinium and Neodymium

Separation of Gd^{3+} and Nd^{3+} investigated using a column contains the prepared material, Cyphos@silica. The column packed with the material loaded by a mixture of both Gd^{3+} and Nd^{3+} ions solution (5.0 mL of 100 mg/L concentration of each). The experiment was performed at flow rate 1 mL/min and bed depth 3 cm. The separation process was first tested for elution of the two metal ions using distilled water and no release of any ions was observed for elution by

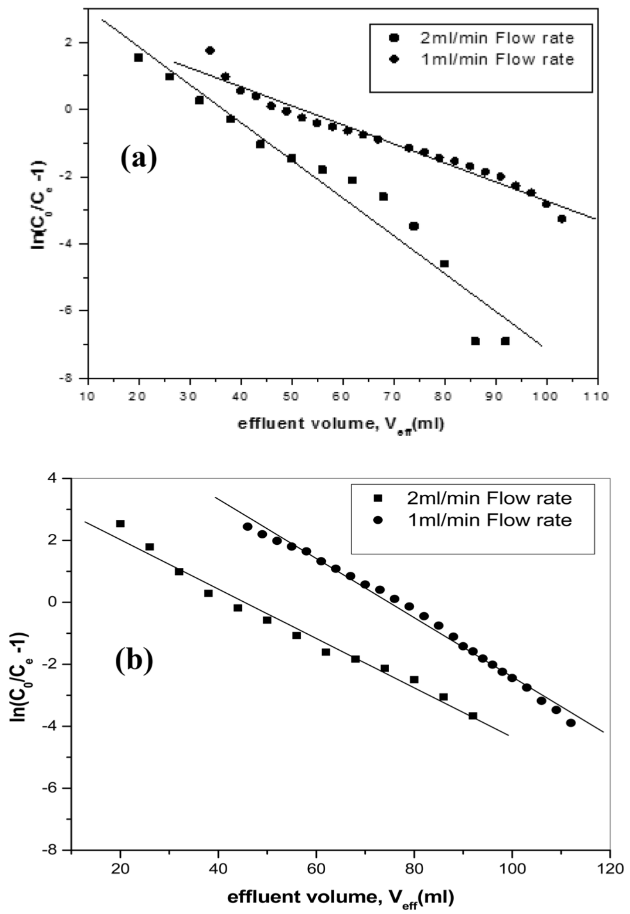

Fig. 8 Thomas model plots for sorption of **a** Nd^{3+} and **b** Gd^{3+} onto cyphos@silica at different flow rates

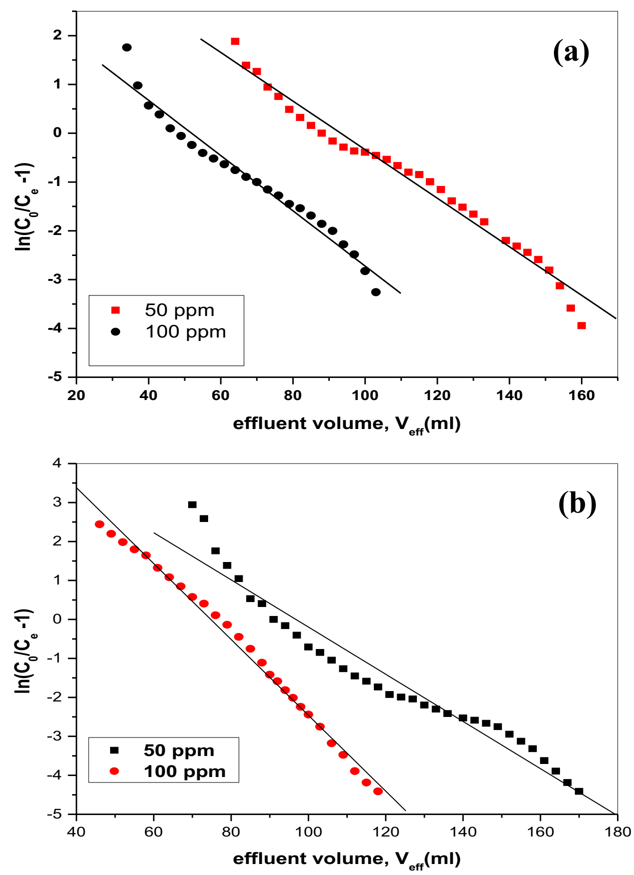

Fig. 9 Thomas model plots for sorption of **a** Nd^{3+} and **b** Gd^{3+} onto cyphos@silica at different initial feed concentrations

distilled water, and also NaOH solution cannot be used due to precipitation of lanthanides in basic media. 1.0 M nitric acid was found to be the best reagent for elution of Gd^{3+} and Nd^{3+}, as shown in Fig. 12.

Comparison of Sorption Capacity of Gd^{3+} and Nd^{3+} on Cyphos@silica with Other Sorbents

The sorption capacity of cyphos@silica toward Gd^{3+} and Nd^{3+} ions was compared to that of few sorbents in the literature, since there are very few investigations that calculated the sorption capacity of neodymium and/or gadolinium ions

Table 5 Thomas model parameters at different conditions for the sorption of Nd^{3+} and Gd^{3+} onto Cyphos@silica: linear regression

	C_0 (mg/L)	Z (cm)	v (mL/min)	K_{Th} (L mg^{-1} min^{-1}) × 10^3	q_0 (mg/g)	R^2	$q_{c\ (exp)}$ (mg/g)
Nd^{3+}							
Exp1	100	2	1	0.882	4.158	0.95	4.8
Exp2	100	3	1	0.566	5.191	0.93	5.6
Exp3	100	3	2	2.251	3.658	0.97	3.5
Exp4	50	3	1	0.497	4.66	0.97	4.86
Gd^{3+}							
Exp1	100	2	1	1.005	6.648	0.98	6.8
Exp2	100	3	1	1.002	7.473	0.99	7.6
Exp3	100	3	2	1.594	4.537	0.98	3.7
Exp4	50	3	1	0.974	4.838	0.94	4.6

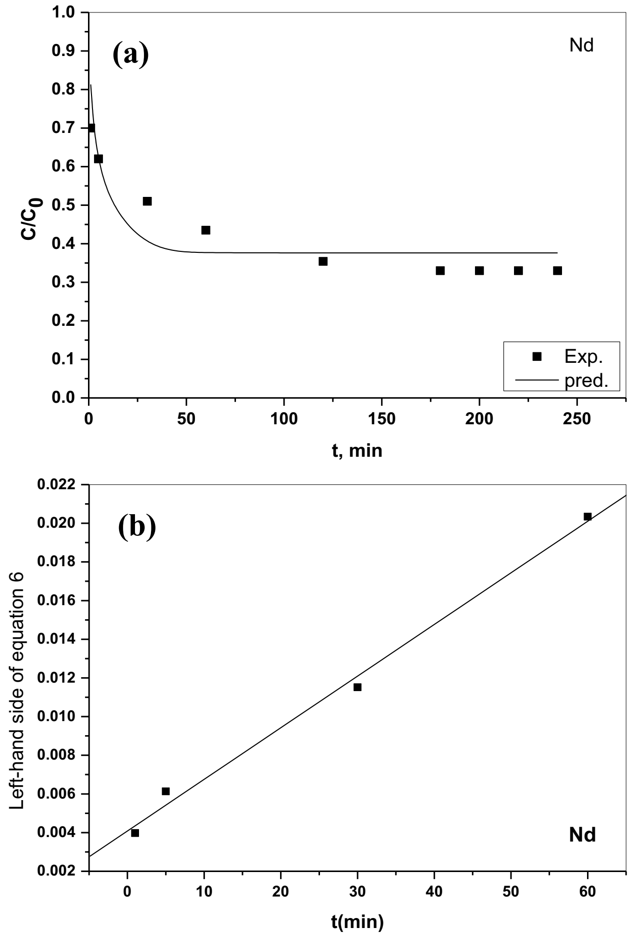

Fig. 10 Kinetic data of Nd^{3+} sorption onto cyphos@silica using Adams–Bohart equation: **a** Eq. 8 and **b** Eq. 10

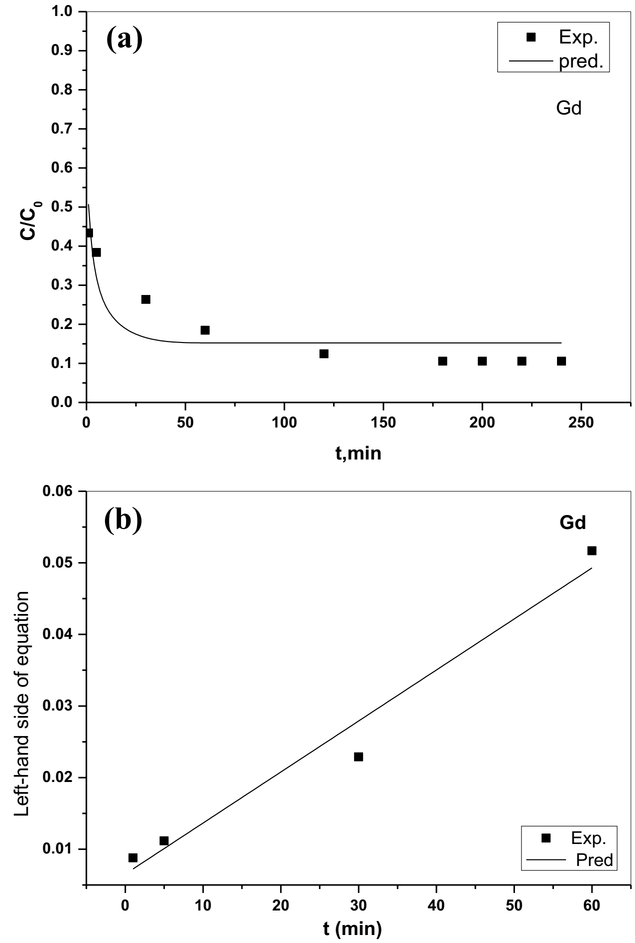

Fig. 11 Kinetic data of Gd^{3+} sorption onto cyphos@silica using Adams–Bohart equations: **a** Eq. 8 and **b** Eq. 10

Table 6 Parameters estimated by fitting the batch kinetic data to non-linear and linear forms of Adam–Bohart equations

Parameters	Metal ions	
	Nd^{3+}	Gd^{3+}
Nonlinear fitting		
k_{AB} (L mg^{-1} min^{-1})	0.0019	0.0063
$q_{0\ pred.}$ (mg/g)	12.47	16.95
$q_{0\ exp}$ (mg/g)	13.40	17.89
Linear fitting		
k_{AB} (L mg^{-1} min^{-1})	0.0003	0.0007

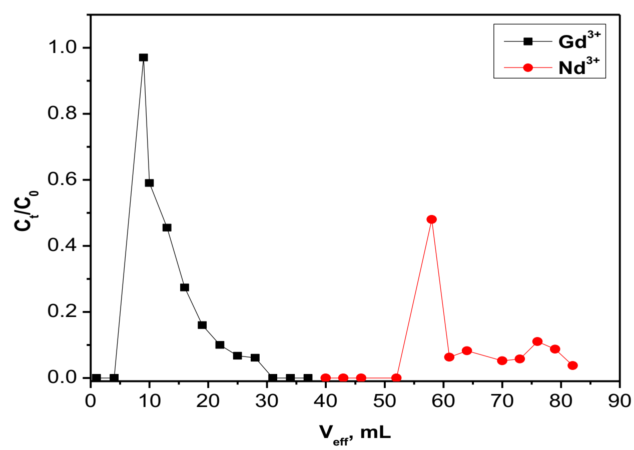

Fig. 12 Separation of Nd^{3+} and Gd^{3+} at 1.0 mL/min flow rate, 3.0 cm bed depth, and 1.0 M HNO_3 medium

using fixed bed column. This gives an importance to this study. Table 6 displays that the cyphos@silica has higher sorption capacity than a sorbent, especially for gadolinium, and others have sorption capacity higher than that of cyphos@silica, but cyphos@silica is characterized by its efficiency for the separation of gadolinium and neodymium ions from each other. While there are many research articles using the batch technique for the removal of Gd^{3+} and

Table 7 Comparison of sorption capacity of Nd^{3+} and Gd^{3+} onto different sorbents

Sorbents	Experimental conditions	Capacity, mg/g		References
		Nd^{3+}	Gd^{3+}	
cyphos@silica	pH = 4.0	5.6	7.6	Present work
Sonicated Emulsion Polymer	pH = 5.0	NR*	16.2	[42]
Phosphorus Functionalized Adsorbent	pH = 6.0	47.5	NR*	[43]
Dowex-HCR-S/S	pH = 4.0	NR*	66.0	[44]
Impregnated Amberlite XAD-4	pH = 5.5	NR*	4.44	[45]

*NR refers to not reported

Nd^{3+} ions. In the previous work [2], the sorption capacity of cyphos@silica obtained from the batch technique was compared with that of other sorbents in the literature, the data revealed that cyphos@silica has much higher sorption capacity than many sorbents. Hence, cyphos@silica is considered as an encouraging sorbent for the removal and separation of gadolinium and neodymium ions (Table 7).

Conclusion

In the present work, separation of Gd^{3+} and Nd^{3+} in was examined in fixed bed mode. Cyphos 104 impregnated silica was used as sorbent. Effect of influent flow rate, bed size, and initial ion concentration on breakthrough curves were considered. It was observed that the sorption capacity was higher at lower flow rate, higher bed depth, and initial ions concentration. The laboratorial data of the column were modeled using Thomas model and Adams–Bohart model. 1.0 M nitric acid was found to be efficient in separating both ions from binary mixture. The experimental data were in good agreement with theoretical results. The study revealed that Cyphos 104 impregnated silica packed in column can be used as an effective sorbent for the removal and separation of Gd^{3+} and Nd^{3+} from aqueous solution.

Compliance with ethical standards

Conflict of interest The authors declare that there is no conflict of interest.

Ethical approval This article does not contain any studies with human participants or animals performed by any of the authors.

References

1. Metwally SS, Hassan RS, El-Masry EH, Borai EH (2018) Gamma-induced radiation polymerization of kaolin composite for sorption of lanthanum, europium and uranium ions from lowgrade monazite leachate. J Radioanal Nucl Chem 315(1):39–49
2. Mohamed WR, Metwally SS, Ibrahim HA, El-Sherief EA, Mekhamer HS, Islam MI, Moustafa, Mabrouk EM (2017) Impregnation of task-specific ionic liquid into a solid support for removal of neodymium and gadolinium ions from aqueous solution. J Molec Liq 236:9–17
3. Metwally SS, Rizk HS (2014) Preparation and characterization of nano-sized iron–titanium mixed oxide for removal of some lanthanides from aqueous solution. Sep Sci Technol 49:2426–2436
4. Charalampides G, Vatalis KI, Apostoplos B, Ploutarch-Nikolas B (2015) Rare earth elements: industrial applications and economic dependency of Europe. Proced Econ Financ 24:126–135
5. Smith CD, Dietz ML (2021) Support loading effects on the performance of an extraction chromatographic resin: toward improved separation of trivalent lanthanides. Talanta 222:121541
6. IAEA-TECDOC-844 (1995) Characteristics and use of Urania-Gadolinia fuels. IAEA, Vienna
7. Shu QA, Khayambashi X, Wei WY (2018) Studies on adsorption of rare earth elements from nitric acid solution with macroporous silica-based bis(2-ethylhexyl) phosphoric acid impregnated polymeric adsorbent. Adsorpt Sci Technol 36(3–4):1049–1065
8. Lee GS, Uchikoshi M, Mimura K, Isshiki M (2010) Separation of major impurities Ce, Pr, Nd, Sm, Al, Ca, Fe, and Zn from La using bis(2-ethylhexyl)phosphoric acid (D2EHPA)-impregnated resin in a hydrochloric acid medium. Sep Purif Technol 71:186–191
9. Gasser MS, Emam ShSh, Rizk SE, Salah BA, Sayed SA, Aly HF (2018) Extraction and separation of uranium (IV) and certain light lanthanides from concentrated phosphoric acid solutions using octyl phenyl acid phosphate. J Molec Liq 272:1030–1040
10. Fryxell GE, Chouyyok WR, Rutledge D (2011) Design and synthesis of chelating diamide sorbents for the separation of lanthanides. J Inorg Chem Commun 14:971–974
11. Gasser MS, El Sherif E, Abdel Rahman RO (2017) Modification of Mg-Fe hydrotalcite using cyanex 272 for lanthanides separation. Chem Eng J 316:758–769
12. Abdel Rahman RO, El Kamash AM, Ali HF, Hung Y-T (2011) Overview on recent trends and developments in radioactive liquid waste treatment part 1: sorption/ion exchange technique. Int J Environ Eng Sci 2(1):1–10
13. Metwally SS, Hassan HS, Samy NM (2019) Impact of environmental conditions on the sorption behavior of ^{60}Co and $^{152+154}Eu$ radionuclides onto polyaniline/zirconium aluminate composite. J Molec Liq 287:110941
14. Metwally SS, Rizk HE, Gasser MS (2017) Biosorption of strontium ions from aqueous solution using modified eggshell materials. Radiochim Acta 105(12):1021–1031
15. Ibrahim HA, Abdel Moamen OA, Abdel Monem N, Ismail IM (2018) Assessment of kinetic and isotherm models for competitive sorption of Cs^+ and Sr^{2+} from binary metal solution onto nanosized zeolite. Chem Eng Commun 205(9):1274–1287
16. El-kamash AM, Borai EH, Goneam Hamed M, Mahmoud A-A (2019) Fixed bed sorption studies on the removal of uranium and

gadolinium ions from aqueous solution using sonicated emulsion polymer. Intern J Innov Res Growth 8(4):20–35
17. Rizk HE, Ahmed IM, Metwally SS (2018) Selective sorption and separation of molybdenum ion from some fission products by impregnated perlite. Chem Eng Process Process Intensif 124:131–136
18. Hamed MM, Hassan RS, Metwally SS (2019) Retardation behavior of alum industrial waste for cationic and anionic radionuclides. Proc Saf Environ Protect 124:31–38
19. Mohammed AA, Abdel OA, Moamen SS, Metwally AM, El-Kamash IA, Al-Geundi MS (2020) Utilization of modified attapulgite for the removal of Sr(II), Co(II), and Ni(II) ions from multicomponent system, part I: kinetic studies. Environ Sci Pollut Res 27:6824–6836
20. Gad HMH, Hamed MM, Abo Eldahab HMM, Moustafa ME, El-Reefy SA (2017) Radiation-induced grafting copolymerization of resin onto the surface of silica extracted from rice husk ash for adsorption of gadolinium. J Molec Liq 231:45–55
21. Ghaly M, El-Sherief EA, Metwally SS, Saad EA (2018) Utilization of nano-cryptomelane for the removal of cobalt, cesium and lead ions from multicomponent system: Kinetic and equilibrium studies. J Hazard Mater 352:1–16
22. Navarro R, Saucedo I, Nnez A, Avila M, Guibal E (2008) Cadmium extraction from hydrochloric acid solutions using Amberlite XAD-7 impregnated with Cyanex 921 (tri-octyl phosphine oxide). React Funct Polym 68:557–571
23. Guibal E, Vincent T, Jouannin C (2009) Immobilization of extractants in biopolymer capsules for the synthesis of new resins: a focus on the encapsulation of tetraalkyl phosphonium ionic liquids. J Mater Chem 19(45):8515–8527
24. Inglezakis V, Fyrillas MM (2017) Adsorption Fixed Beds Modeling Revisited; Generalized Solutions for S-Shaped Isotherms. Chem Eng Commmun 204(11):1299–1317
25. Nishihama S, Kohata K, Yoshizuka K (2013) Separation of lanthanum and cerium using a coated solvent-impregnated resin. Sep Purif Technol 118:511–518
26. Wei S, Liu J, Zhang S, Chen X, Liu Q, Zhu L, Guo L, Liu X (2016) Stoichiometry, isotherms and kinetics of adsorption of In(III) on Cyanex 923 impregnated HZ830 resin from hydrochloric acid solutions. Hydrometal 164:219–227
27. Valls RG, Hrdlicka A, Perutka J, Havel J, Deorkar NV, Tavlarides LL, Muñoz M, Valiente M (2001) Separation of rare earth elements by high performance liquid chromatography using a covalent modified silica gel column. Anal Chim Acta 439:247–253
28. Yue Zhou W, Xin Peng W, Rui Qin L, Yan W, Shigekazu U, Tsuyoshi A (2012) An advanced partitioning process for key elements separation from high level liquid waste. Sci China Chem 55(9):1726–1731
29. El-Kamash AM (2008) Evaluation of zeolite-A for the sorptive removal of Cs^+ and Sr^{2+} ions from aqueous solutions using batch and fixed bed column operations. J Hazard Mater 151:432–445
30. Trikha R, Sharma BK, Sabharwal KN, Prabhu K (2015) Elution profiles of lanthanides with α-hydroxyisobutyric acid by ion exchange chromatography using fine resin. J Sep Sci 38(21):3810–3814
31. Metwally SS, El-Sherief EA, Mekhamer HS (2020) Fixed-bed column for the removal of cesium, strontium, and lead ions from aqueous solutions using brick kiln waste. Sep Sci Technol 55(4):635–647
32. Bohart GS, Adams EQ (1920) Some aspects of the behavior of charcoal with respect to chlorine. J Chem Soc 42:523–529
33. Duga BNDF, Imperial PEA, Soriano AN, Nieva AD (2016) Packed bed biosorption of lead and copper ions using sugarcane. ASEAN J Chem Eng 16(1):23–37
34. Thomas HC (1944) Heterogenous ion exchange in flowing system. J Am Chem Soc 66:1466–1664
35. Dalia Saad M, Cukrowska E, Tutu H (2015) Column adsorption studies for the removal of U by phosphonated cross-linked polyethylenimine: modelling and optimization. Appl Water Sci 5:57–63
36. Technical reports series No. 408 (2002) Application of ion exchange processes for the treatment of radioactive waste and management of spent ion exchangers. International Atomic Energy Agency, Vienna
37. Jolley RL, Dole LR, Godbee HW, Kibbey AH, Oyen LC, Robinson SM, Rodgers BR, Tucker RF (1985) Low-Level Radioactive Waste From Commercial Nuclear Reactors, Report, program managed through the U.S. Department of Energy
38. Likozar B, Senica D, Pavko A (2012) Comparison of adsorption equilibrium and kinetic models for a case study of Pharmaceutical active ingredient Adsorption from fermentation broths: parameter determination, simulation, Sensitivity analysis and optimization. Brazilian J Chem Eng 29:635–652
39. Hoong Chu K, Yong Kim E, Feng X (2011) Batch kinetics of metal biosorption: application of the Bohart-Adams rate law. Sep Sci Technol 46:1591–1601
40. Loebenstein WV (1962) Batch adsorption from solution. J Res Natl Bur Std A Phys Chem 66A:503–515
41. Loebenstein WV (1963) Adsorption, desorption, resorption. J Res Natl Bur Std A Phys Chem 67A(6):615–624
42. El-kamash AM, Borai EH, Hamed MG, Abo-Aly MM (2019) Fixed bed sorption studies on the removal of uranium and gadolinium ions from aqueous solution using sonicated emulsion polymer. Intern J Innovative Res Grow 8(4):20–35
43. Park H-J, Tavlarides LL (2010) Adsorption of neodymium(III) from aqueous solutions using a phosphorus functionalized adsorbent. Ind Eng Chem Res 49:12567–12575
44. Hamed MM, Rizk SE, Nayl AA (2016) Adsorption kinetics and modeling of gadolinium and cobalt ions sorption by an ion-exchange resin. Particul Sci Technol 34(6):716–724
45. El-Sofany EA (2008) Removal of lanthanum and gadolinium from nitrate medium using Aliquat-336 impregnated onto Amberlite XAD-4. J Hazard Mater 153:948–954